agronomy

MDPI

Article

Topography Controls N_2O Emissions Differently during Early and Late Corn Growing Season

Waqar Ashiq [1], Hiteshkumar B. Vasava [1], Uttam Ghimire [2], Prasad Daggupati [2] and Asim Biswas [1,*]

[1] School of Environmental Sciences, University of Guelph, Guelph, ON N1G 2W1, Canada; washiq@uoguelph.ca (W.A.); hvasava@uoguelph.ca (H.B.V.)
[2] School of Engineering, University of Guelph, Guelph, ON N1G 2W1, Canada; ughimire@uoguelph.ca (U.G.); pdaggupa@uoguelph.ca (P.D.)
* Correspondence: biswas@uoguelph.ca; Tel.: +1-519-824-4120 (ext. 54249); Fax: +1-519-837-0756

Abstract: Topography affects soil hydrological, pedological, and biochemical processes and may influence nitrous oxide (N_2O) emissions into the atmosphere. While N_2O emissions from agricultural fields are mainly measured at plot scale and on flat topography, intrafield topographical and crop growth variability alter soil processes and might impact N_2O emissions. The objective of this study was to examine the impact of topographical variations on crop growth period dependent soil N_2O emissions at the field scale. A field experiment was conducted at two agricultural farms (Baggs farm; BF and Research North; RN) with undulating topography. Dominant slope positions (upper, middle, lower and toeslope) were identified based on elevation difference. Soil and gas samples were collected from four replicated locations within each slope position over the whole corn growing season (May–October 2019) to measure soil physio-chemical properties and N_2O emissions. The N_2O emissions at BF ranged from -0.27 ± 0.42 to 255 ± 105 g ha^{-1} d^{-1}. Higher cumulative emissions were observed from the upper slope (1040 ± 487 g ha^{-1}) during early growing season and from the toeslope (371 ± 157 g ha^{-1}) during the late growing season with limited variations during the mid growing season. Similarly, at RN farm, (emissions ranged from -0.50 ± 0.83 to 70 ± 15 g ha^{-1} d^{-1}), the upper slope had higher cumulative emissions during early (576 ± 132 g ha^{-1}) and mid (271 ± 51 g ha^{-1}) growing season, whereas no impact of slope positions was observed during late growing season. Topography controlled soil and environmental properties differently at different crop growth periods; thus, intrafield variability must be considered in estimating N_2O emissions and emission factor calculation from agricultural fields. However, due to large spatial variations in N_2O emissions, further explorations into site-specific analysis of individual soil properties and their impact on N_2O emissions using multiyear data might help to understand and identify hotspots of N_2O emissions.

Keywords: climate change; greenhouse gases; spatiotemporal variation of nitrous oxide; crop growth; elevation; slope

check for updates

Citation: Ashiq, W.; Vasava, H.B.; Ghimire, U.; Daggupati, P.; Biswas, A. Topography Controls N_2O Emissions Differently during Early and Late Corn Growing Season. *Agronomy* **2021**, *11*, 187. https://doi.org/10.3390/agronomy11010187

Received: 24 December 2020
Accepted: 14 January 2021
Published: 19 January 2021

Publisher's Note: MDPI stays neutral with regard to jurisdictional claims in published maps and institutional affiliations.

Copyright: © 2021 by the authors. Licensee MDPI, Basel, Switzerland. This article is an open access article distributed under the terms and conditions of the Creative Commons Attribution (CC BY) license (https://creativecommons.org/licenses/by/4.0/).

1. Introduction

Nitrous oxide (N_2O) is a potent greenhouse gas (GHG) with 298 times more global warming potential than carbon dioxide and contributes to climate change [1]. Each economic sector releasing GHGs into the atmosphere including agriculture must take responsibility for reducing their contribution following the Kyoto Protocol and Paris agreement within the United Nations Framework Convention on Climate Change (UNFCCC) [2–4]. Agriculture, forestry, and other land use is the second largest source of GHG emissions after the energy sector and contributes approximately 81% of the global [5,6] and 77% of Canadian anthropogenic N_2O emissions [7]. Agricultural management practices (such as nutrient management, inclusion of cover crops, tillage, and soil amendments) have been known to affect and regulate soil N_2O emissions [8–10]. The application of inorganic nitrogen (IN) fertilizer alone accounts for 13% of global agricultural N_2O emissions [11]. Soil N_2O emission is the result of complex interactions among soil biogeophysicochemical

properties, including soil temperature, moisture, pH, EC, soil organic matter (SOM), and IN that affect soil processes including nitrification and denitrification [12–19]. Topographical variations in agricultural fields affect soil hydrological and pedological processes which regulate soil physicochemical properties, crop growth and impact nitrous oxide emissions from agricultural landscape [20–25]. Saggar et al., [25] evaluated the impact of urine and dung deposition from grazing animals on N_2O emissions from a hilly pasture. However, the spatial distribution of dung and urine by grazing animals is not uniform over the field which can mask the actual impact of topographical variations on nutrient distribution and N_2O emission. Corre et al., [20] studied the role of topographical variations on N_2O emissions from different land uses, however, only two slope positions were sampled (shoulder and footslope). Additionally, sampling points were randomly selected without consideration of soil and slope properties. Gu et al., [21] evaluated the role of only two slope positions (shoulder and footslope) on N_2O emissions from winter wheat, however, the sampling was carried out only for two months which limits the evaluation of the integrated impact of crop and topography on N_2O emissions. Vilain et al., [22] studied the N_2O emissions from different slope positions. However, this study was carried out (i) along a transect, (ii) sampling points were selected randomly and, iii) shoulder and footslope positions were located in separate fields with different land uses. As land-use variations impact N_2O emissions, so actual estimation of the role of topography could not be evaluated if all sampling locations or topographical positions are not located within the same land use. Temporal variations in N_2O emissions as crops grow have been widely studied [26–28] however, the impact of topography during different crop growth periods has not been considered though it might impact water and nutrient translocation along with slope positions and might trigger a divergent spatial and temporal response in N_2O emissions.

Different topographic indices, such as elevation and slope positions in agricultural fields, can strongly influence spatial variation in soil physicochemical properties [29–34]. For example, topographical heterogeneity can affect nutrient flow within the landscape and nutrients from top slope positions can be transported and translocated to the downslope and toeslope positions [30,33,35–37] which can alter soil microbial activity, nutrient and biogeochemical cycles and thus, biomass production across agricultural fields [38–40]. The topography-mediated redistribution of water, energy, and nutrients within the landscape can affect underlying soil N_2O emissions processes. Additionally, the N_2O emission factors (EFs) for agricultural soils used by the Intergovernmental Panel on Climate Change (IPCC) account for the application of IN fertilizer, animal manure, decomposition of crop residues, and biological nitrogen fixation [6,41,42]. However, topographical variations (e.g., slope, wetness index, elevation) in agricultural landscapes are not considered in EF calculations although they have strong control on soil hydrological, pedological, and biogeochemical processes and thus, N_2O emissions from soil [43–46]. Furthermore, management practices and crop growth stages interact with topography affecting water and nutrient movement across slope which might increase denitrification at footslope positions resulting in increased N_2O emissions or might result in complete denitrification producing nitrogen [47]. Interannual and intercrop variations in soil and crop parameters have been investigated and have indicated the strong impact of temporal variations of soil properties on crop yield [48]. However, intraseason variations during the crop growth season (early, mid, and late growth period) also impact soil physicochemical properties due to variations in land cover and environmental conditions which might impact soil N_2O emissions. Topography, a dominant soil forming factor [49], can alter other soil forming factors and processes and create strong variations in soil properties in different crop growth periods [50–52] that may affect N_2O emissions at the landscape level. The impact of these variations on N_2O emissions had been studied previously [21,22,34,53–57]. However, most of these studies were either conducted along a transect [21,22,53–55] or in forest or pastures [34,57] while annual crops receiving intense management practices can contribute largely to N_2O emissions. Additionally, the sampling points in these studies were randomly selected

without prior consideration of soil topographical variations and soil classification leading to unidentified variations that may have impacted the results.

Most of the agricultural fields in temperate regions have undulating landscapes. However, estimation of N_2O emissions from agricultural soils and EFs for GHG inventories were performed on flat and homogenized plots which may lead to erroneous results. For accurate estimation of N_2O emissions and EFs from highly variable agricultural landscapes, the effect of topographical variations on crop growth period dependent N_2O emissions must be quantified at field scale. The overall objective of this study was to examine the impact of topographical variations on crop growth period dependent soil N_2O emissions from agricultural fields. The specific objectives were (1) to examine the impact of different slope positions on soil physicochemical properties (e.g., soil temperature, moisture, pH, EC, NO_3^-, and NH_4^+) and (2) to determine spatiotemporal variations in N_2O emissions during different crop growth periods at field scale. We hypothesized that topographic variability in agricultural fields such as slope positions (toeslope, lower slope, middle slope, upper slope) control variations in underlying soil processes that are represented as the variations in soil physicochemical properties. The variation in soil properties and processes can impact the delivery of substrates and/or conditions required for N_2O emission processes at different landscape positions at different growth periods.

2. Materials and Methods

2.1. Experimental Site and Crop Management

A field experiment was conducted at two agricultural farms with undulating landscapes (Baggs farm and Research North farm) near Cambridge, Ontario, Canada. Baggs farm is located at 43° 27′ 35″ N, 80° 18′ 35″ W, and Research North is located at 43° 26′ 25″ N and 80° 20′ 45″ W. The soil texture at Baggs farm and Research North is sandy loam (sand:silt:clay = 59 ± 5:32 ± 4:8 ± 4) and loamy sand (sand:silt:clay = 76 ± 2:18 ± 1:6 ± 2), respectively. According to Köppen climate classification, the area had humid continental climate. The total area selected for this study at Baggs farm was 1.22 ha while at Research North, the field scale watershed was delineated using digital elevation data measuring 2.21 ha. Lidar Digital Terrain Model Land Information Ontario data set was processed to obtain slope and topographical wetness index (TWI) in ArcGIS 10.6.1 (ESRI) and Pennock soil classification [58] was performed with System for Automated Geoscientific Analyses (SAGA-GIS) software, an open-source geographic information system software, available online at http://www.saga-gis.org/en/index.html). Initially, the selected area at each farm was divided into different topographical positions or clusters based on digital elevation model. Baggs farm was divided into 3 slope positions (toeslope, middle slope, and upper slope) with 4 sampling points in each position as replicates (total 12 sampling points), while Research North was divided into 4 slope positions with 4 sampling points in each position as replicates (total 16 sampling points) (Figure 1). Traditionally, replicates are randomly selected within a block (here slope position) assuming uniform soil conditions. However, spatial heterogeneity in soil properties within a block could increase the error. Therefore, we used conditional Latin Hypercube sampling (cLHS) design implemented in R statistical package to select 4 replicates within each slope position using available soil data (digital elevation, TWI, slope, and Pennock soil classes as covariates) to capture maximum spatial variation within each slope position.

Corn hybrid Pioneer A6455G8 RIB (2825 corn heat units, glyphosate-tolerant) was grown for grain purposes at both farms without artificial irrigation. Both farms were planted with wheat in 2018. Urea and Muriate of Potash were broadcasted one day before tillage providing N:P:K:S = 104:0:34:0 kg ha^{-1}. Fields were tilled with disc harrow (Sunflower 1233) to a depth of 10 cm one day before planting. Corn was planted at 76,600 seeds ha^{-1}, with a row spacing of 0.75 m on 17 May 2019 at Baggs farm and 19 May 2019 at Research North. At the time of planting, Monoammonium Phosphate and Sulfate of Potash fertilizers were applied using a corn planter (N:P:K:S = 8:38:76:27 kg ha^{-1}). A subsequent fertilizer dose (N:P:K:S = 78:0:0:14 kg ha^{-1}) in the form of Ammonium

Thiosulfate and Urea Ammonium Nitrate mixture (ATS:UAN = 18:82) was side dressed 6 cm away from corn rows on 6 July 2019 at Baggs farm and 07 July 2019at Research North. Weed control was achieved using glyphosate post-emergence application at 2.47 L ha^{-1} using a boom sprayer on 18 June 2019. Corn was harvested on 9 November 2019 at Baggs farm and 17 November 2019at Research North.

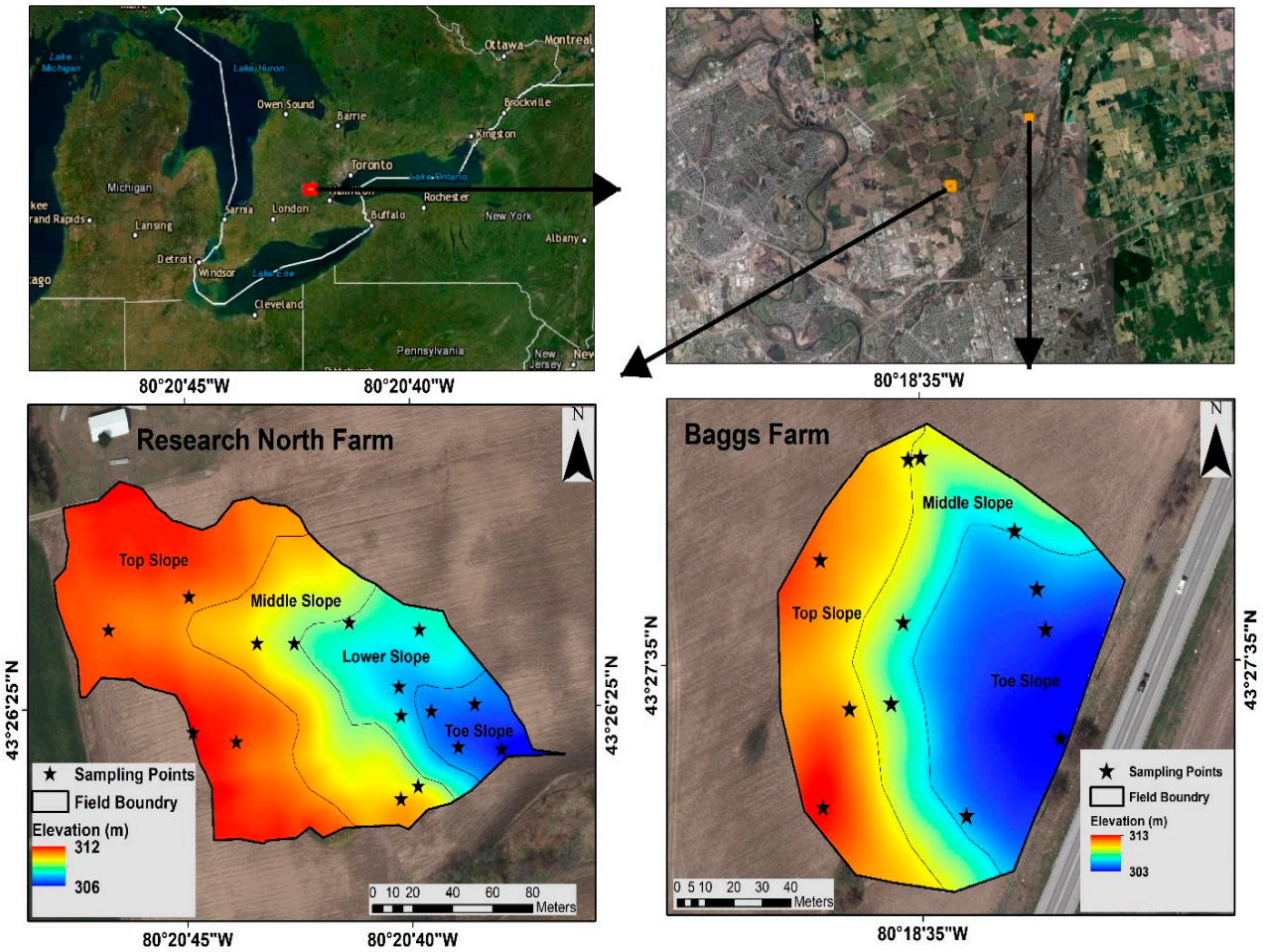

Figure 1. Location of Research North and Baggs farm.

Corn plant undergoes various physiological changes which are divided mainly into vegetative (VE, V3, V5, V12, V18, VT) and reproductive stages (R1, R2,...R6) [59]. During the early growing season (VE–V5), there is less demand for plant N uptake until a sufficient stand is established which might increase N losses. During the mid growing season (V6–R1), active vegetative growth requires higher amounts of water and nutrients and increases their uptake from soil and plants when they enter the reproductive stage. During the late growing season (R2–R6), the plant completes grain filling and reaches physiological maturity. The whole growth period was divided into early, mid, and late growing season for soil and gas sampling on 11 occasions at Baggs farm and 12 occasions at Research North. Soil and gas samples were collected from the Baggs farm during early season (26 May, 3 June), mid season (21 June, 4 July, 9 July, 23 July, 9 August) and late growing season (23 August, 9 September, 25 September, 10 October) and from Research North during early (22 May, 26 May, 6 June), mid (21 June, 5 July, 11 July, 18 July, 7 August), and the late growing season (20 August, 5 September, 24 September, 11 October).

2.2. Gas and Soil Sampling

Gas samples were collected using static enclosed chambers. The sampling chamber consisted of two units (a collar and lid): (a) the collar, a polyvinyl chloride (PVC) open cylinder (inner diameter = 44.2 cm, outer diameter = 45.7 cm, and height = 19 cm) which was inserted between corn rows to a depth of 10 cm at each sampling location; (b) a PVC lid with 8.3 cm height, covered with round PVC sheet (1.27 cm thick) fixed into positions using PVC cement [60]. The lids were covered with insulating double-layered reflective bubble wrap. The lid had 4 clamps on sides to lock it to collar during gas sampling. The bottom of the lid had a groove with a rubber septum to prevent gas leakage. The lid was deployed on the top of each collar and clamps were locked during gas sample collection. Collar height above the soil surface was measured at each gas sampling date and the total volume of the sampling chamber was calculated. The Chamber lid had tubing outlets connected to an internal four-port manifold, made of polypropylene union tees and four tubes (15 cm long by 0.15 cm internal diameter) (Chemfluor FEP, Cole-Parmer) to collect the samples from four points within the headspace ensuring a representative sample. A 10 cm long and 0.48 cm inner diameter vent tube was connected to the lid to compensate for inner and outer air pressure [60]. For each measurement, four gas samples were taken from the chamber using a 20 mL non-sterile syringe at 10 min intervals (0, 10, 20, and 30 min after closure) [61]. To minimize any effect of diurnal variations in emissions, the samples were collected between 0900 and 1200 h on each sampling day [62]. The gas samples were transferred to 12 mL evacuated clear glass vials sealed with gas-tight neoprene septum (Labco). The N_2O in gas sample was measured using gas chromatography (BRUKER-GC450) [61] and daily flux was calculated based on the change in N_2O concentration with time using all time points sampled by following Equation (1).

$$F = \frac{dC}{dt}\frac{V}{A}\frac{pM}{RT}k \quad (1)$$

where dC/dt is the rate of change of N_2O concentration over time or slope of the linear equation (μg N_2O g^{-1} air s^{-1}), V is the headspace volume of the chamber (m^3), A is the land surface area covered by the chamber (m^2), p is the barometric pressure (Pa = J m^{-3}), M is the molar mass of N_2O (44.013 g mol^{-1}), R is the universal gas constant (8.314 J mol^{-1} K^{-1}), T is the absolute temperature (K) around sampling chamber and K is a conversion factor (864 mg μg^{-1} m^2 ha^{-1} s h^{-1}) to convert values to g ha^{-1} d^{-1} [63,64]. Soil and air temperature were monitored at the same time as gas sampling at four places around each sampling chamber. Soil temperature was measured with a soil thermometer from a depth of 10–15 cm. Atmospheric pressure values were obtained from Environment Canada website from Waterloo International airport weather station.

Soil samples were collected at four places around the static chambers at each gas sampling date using a soil auger from 0–15 cm depth, sealed in marked plastic bags and stored at −20 °C. Soil gravimetric moisture was determined after oven drying the soil sub-samples at 105 °C. Extraction of field moist soil was carried out using 2 M KCl solution. All sample weights were converted to oven-dry weight (105 °C). The concentration of NO_3^- and NH_4^+ was determined using a SEAL-AA3HR Autoanalyzer at the soil laboratory of the School of Environmental Sciences, University of Guelph. Soil extraction and calculations of NO_3^- and NH_4^+ were performed following [65]. Soil pH and EC were determined from air-dried, sieved soil samples using Fisher Scientific Accumet XL600 m (Fisher Scientific, Hampton, New Hampshire). For pH and EC, 30 mL deionized water was added to 15 g air dried soil in a 50 mL centrifuge plastic tube and shaken for 60 min. The solution was kept for 1 h to allow the soil to settle and the pH before measuring pH [65]. Soil EC was measured from the clear supernatant of the same soil mixture after the soil particles settled to the bottom of the tube [65].

2.3. Data Analysis

Daily N_2O fluxes were calculated using Microsoft Office Excel 2016 (Microsoft, Inc., Washington, WA, USA). It was assumed that N_2O emissions between 0900 and 1200 h on each sampling date were the average of the daily N_2O flux [62,64]. Cumulative N_2O emissions were calculated by multiplying the average fluxes of two successive determinations by the length of the period between samplings and adding that amount to the previous cumulative total [26,66] using following Equation (2).

$$\text{Cumulative flux} = \sum_{i=1}^{n} (F_i + F_{i+1}) /2 \times (t_{i+1} - t_i) \times 24 \quad (2)$$

where F is the N_2O flux (g ha^{-1} d^{-1}), i is the ith measurement, the term of $(t_{i+1} - t_i)$ is the days between two adjacent sampling events, and n is the total number of sampling events [67,68]. Statistical analyses were performed with Minitab® Statistical Software ((Version 19, Minitab Inc., Pennsylvania, PA, USA)). The effects of different slope positions on soil N_2O emissions during different corn growth stages were assessed using two-way analyses of variance (ANOVA), followed by least significant difference test (LSD); $p < 0.05$ was considered statistically significant. Daily N_2O fluxes and cumulative emissions at BF (shown in Tables 1 and 2, respectively) and RN (Tables 3 and 4, respectively) were prepared using mean values (mean ± SEM) from four replications at each slope position. Figures showing temporal changes in soil properties and N_2O emissions were prepared using SigmaPlot 12 (Systat Software Inc., San Jose, CA, USA). Multiple scatter plots were prepared using mean data from all replications (4) for each slope position (Mean ± SEM).

Table 1. Soil N_2O emissions (g ha^{-1} d^{-1}) from different slope positions at different sampling dates during early, mid, and late growing season (2019) from Baggs farm. Means sharing different letters in each season are significantly different from each other (LSD, $p < 0.05$).

	Early Season			Mid Season					Late Season		
	26 May	**3 June**	**21 June**	**4 July**	**9 July**	**23 July**	**9 August**	**23 August**	**9 September**	**25 September**	**10 October**
Toeslope	166.8 ± 45^{ab}	26.6 ± 10^{b}	5.8 ± 1.2^{ab}	3 ± 0.7^{abcd}	2.5 ± 0.7^{bcd}	3.8 ± 0.9^{abcd}	1.9 ± 1.1^{cd}	3.1 ± 2^{ab}	7.4 ± 2.3^{a}	3.9 ± 2.8^{ab}	2.9 ± 2^{ab}
Middle slope	135.3 ± 41^{ab}	18.6 ± 5^{b}	6.6 ± 1^{a}	2.5 ± 0.7^{bcd}	2.3 ± 0.4^{bcd}	4.9 ± 2.8^{abcd}	1.5 ± 0.3^{d}	1.2 ± 0.2^{b}	0.2 ± 0.3^{b}	0.8 ± 0.1^{b}	0.5 ± 0.1^{b}
Upper slope	254.8 ± 105^{a}	6 ± 1.1^{b}	4.1 ± 1.3^{abcd}	3.2 ± 0.5^{abcd}	2.2 ± 0.4^{bcd}	5.4 ± 1.8^{abc}	1.8 ± 0.5^{cd}	0.8 ± 0.3^{b}	-0.3 ± 0.4^{b}	1.0 ± 0.6^{b}	1.6 ± 0.9^{b}

Analysis of Variance

	Early Season					Mid Season					Late Season				
	*** DF**	**SS**	**MS**	**F**	**P**	**DF**	**SS**	**MS**	**F**	**P**	**DF**	**SS**	**MS**	**F**	**P**
Slope position	2	11,692	5846	0.4	0.678	2	0.5	0.2	0.03	0.967	2	139	70	7	0.003
Sampling date	1	170,495	170,495	11.6	0.004	4	122	31	4.2	0.006	3	4.5	1.5	0.2	0.926
Slope position × Sampling date	2	19,886	9943	0.7	0.522	8	19	2.38	0.3	0.951	6	56	9	1	0.456

* DF = degree of freedom, SS = sum of squares, MS = mean square, F = F-statistic, P = the probability of obtaining an F statistic.

Table 2. Soil cumulative N_2O emissions (g ha^{-1}) from different slope positions during early (26 May to 3 June), mid (21 June to 9 August), and late growing season (23 August to 10 October) during 2019 from Baggs farm. Means sharing different letters are significantly different from each other (LSD, $p < 0.05$).

	Early Growing Season	**Mid Growing Season**	**Late Growing Season**
Toeslope	760 ± 240^{ab}	239 ± 46^{bc}	371 ± 157^{bc}
Middle slope	606 ± 212^{abc}	261 ± 80^{bc}	82 ± 15^{c}
Upper slope	1040 ± 487^{a}	229 ± 17^{bc}	68 ± 20^{c}

Analysis of Variance

	DF	**SS**	**MS**	**F**	**P**
Slope positions	2	145,771	72,885	0.4	0.659
Growing season	2	2,849,227	1,424,613	8.3	0.002
Slope positions × Growing season	4	476,920	119,230	0.7	0.603

DF = degree of freedom, SS = sum of squares, MS = mean square, F = F-statistic, P = the probability of obtaining an F statistic.

Table 3. Soil N_2O emissions (g ha^{-1} d^{-1}) from different slope positions at different sampling dates during early, mid and late growing season (2019) from Research North farm. Means sharing different letters in different growing seasons are significantly different from each other (LSD, $p < 0.05$).

	Early Season				Mid Season					Late Season		
	22 May	**26 May**	**6 June**	**21 June**	**5 July**	**11 July**	**18 July**	**7 August**	**20 August**	**5 September**	**24 September**	**11 October**
Toeslope	23 ± 14^{b}	26 ± 3^{b}	8.2 ± 2.3^{b}	3 ± 0.3^{cd}	1.5 ± 0.1^{d}	0.5 ± 0.4^{d}	4.4 ± 1.6^{abcd}	1.2 ± 0.3^{d}	1.5 ± 1^{ab}	0.3 ± 0.2^{b}	0.3 ± 0.4^{ab}	-0.5 ± 0.8^{b}
Lower slope	8.4 ± 1.4^{b}	59 ± 13^{a}	16.2 ± 7.8^{b}	2.7 ± 0.6^{cd}	0.3 ± 0.2^{d}	1 ± 0.2^{d}	9.6 ± 2.5^{ab}	1.7 ± 0.3^{d}	1.3 ± 0.4^{ab}	0.01 ± 0.2^{b}	$2.5 \pm 2b^{a}$	0.1 ± 0.4^{b}
Middle slope	7.9 ± 1.6^{b}	52 ± 5^{a}	15 ± 4.3^{b}	3 ± 0.4^{cd}	2 ± 0.2^{cd}	2.2 ± 0.5^{cd}	10 ± 6.1^{a}	2.4 ± 1.3^{cd}	1.4 ± 0.1^{ab}	0.3 ± 0.2^{b}	0.3 ± 0.2^{b}	1.2 ± 0.3^{ab}
Upper slope	7.1 ± 2^{b}	70 ± 15^{a}	12.9 ± 2^{b}	4.3 ± 1.2^{bcd}	3.3 ± 1.3^{cd}	0.1 ± 1.3^{d}	7.7 ± 1.9^{abc}	4.1 ± 1.7^{bcd}	1.3 ± 0.3^{ab}	1.0 ± 0.3^{ab}	1.0 ± 0.2^{ab}	1.6 ± 0.7^{ab}

Analysis of Variance

	Early Season					Mid Season					Late Season				
	DF	**SS**	**MS**	**F**	**P**	**DF**	**SS**	**MS**	**F**	**P**	**DF**	**SS**	**MS**	**F**	**P**
Slope position	3	793	264	0.8	0.488	3	45	15	0.9	0.444	3	5.8	1.9	0.8	0.521
Sampling date	2	16,882	8441	26.4	0.000	4	486	122	7.3	0.000	3	9.6	3.2	1.3	0.295
Slope position × sampling date	6	4190	698	2.2	0.069	12	89	7	0.5	0.937	9	21.6	2.4	1.0	0.489

DF = degree of freedom, SS = sum of squares, MS = mean square, F = F-statistic, P = the probability of obtaining an F statistic.

Table 4. Soil cumulative N_2O emissions (g ha^{-1}) from different slope positions during early (22 May to 6 June), mid (21 June to 7 August), and late growing season (20 August to 11 October) during 2019 from Research North farm. Means sharing different letters are significantly different from each other (LSD, $p < 0.05$).

	Early Growing Season	**Mid Growing Season**	**Late Growing Season**
Toeslope	276 ± 50^{bc}	152 ± 23^{c}	86 ± 64^{c}
Lower slope	521 ± 154^{a}	214 ± 39^{c}	115 ± 48^{c}
Middle slope	466 ± 40^{ab}	259 ± 107^{bc}	93 ± 8^{c}
Upper slope	576 ± 132^{a}	271 ± 51^{bc}	118 ± 27^{c}

Analysis of Variance

	DF	**SS**	**MS**	**F**	**P**
slope positions	3	147,906	49,302	2.15	0.113
growing season	2	1,052,181	526,091	22.89	0.000
slope positions × growing season	6	93,529	15,588	0.68	0.668

DF = degree of freedom, SS = sum of squares, MS = mean square, F = F-statistic, P = the probability of obtaining an F statistic.

3. Results and Discussion

3.1. Soil Physicochemical Properties

3.1.1. Soil Temperature and Moisture

At Baggs farm, the toeslope had lower soil temperature (16.8 ± 0.3 °C) and higher gravimetric moisture content (0.16 ± 0.3 g g^{-1}) as compared to middle and upper slopes. Average soil temperature during the early growing season was 15.7 ± 0.2 °C, which increased to 20.7 ± 0.2 °C during the midseason and dropped to 15.2 ± 0.2 °C in the late growing season. Whereas soil had higher soil moisture content during the early growing season 0.19 ± 0.02 followed by mid (0.13 ± 0.02), and late season (0.11 ± 0.02) (Figure 2a,b). At Research North, soil had lower temperature at the toe and middle slopes and higher moisture (at middle slope) as compared to other slope positions. When examining growing seasons, the mid growing season had the maximum soil temperature (23.1 ± 0.3 °C), and lowest soil moisture content (0.078 ± 0.01) (Figure 3a,b). Water accumulation at the toeslope increased soil moisture content and decreased soil temperature as compared to the middle and upper slopes [69–71]. Higher moisture during the early growing season at both farms could be attributed to higher amounts of stored water in the soil due to spring snowmelt and rainfall during the early growing season (31.8 mm) (Figure 4b). Seasonal changes in soil moisture content at different landscape positions may be due to variations in depth of A and B horizons, patterns of vertical and lateral hydraulic gradient, and fluctuations in groundwater depth caused by snowmelt, precipitation, slope flux, and groundwater recession from evapotranspiration [72–74].

3.1.2. Soil pH and EC

At Baggs farm, the lowest soil pH (7 ± 0.1) was observed during the early growing season followed by a slight increase (7.4 ± 0.1) during the midseason which remained stable in the late growing season. Over the whole season, soil pH increased at the toeslope from 7.07 ± 0.1 to 7.36 ± 0.1, at the mid slope from 7.04 ± 0.1 to 7.38 ± 0.1, and at the upper slope from 6.97 ± 0.1 to 7.37 ± 0.1 (Figure 2d). At Research North, the lowest soil pH was recorded during the early growing season (6.97 ± 0.07), which increased to (7.45 ± 0.07) in the mid growing season with a slight decrease in the late growing season (7.40 ± 0.08) (Figure 3d). Over the whole growing season, pH increased at the toeslope from 6.94 ± 0.06 to 7.36 ± 0.1, at the lower slope from 7.03 ± 0.05 to 7.44 ± 0.05, at the middle slope from 6.95 ± 0.1 to 7.40 ± 0.07, and at the upper slope form 6.98 ± 0.08 to 7.40 ± 0.08. An overall increase in soil pH was observed after the Urea application at planting. Soil pH again increased after the 2nd dose of Ammonium Thiosulfate application on 6 July at the Baggs farm and 7 July at Research North. Urea was broadcast and incorporated into the soil which increased the rate of hydrolysis and produced a mixture of NH_3, NH_4^+, HCO_3^-, and CO_3^- which also might have contributed to the increase in soil pH [76,77]. Higher soil moisture content at the toeslope increased leaching and a reduction in soluble base cations leading to higher H^+ activity resulting in lower soil pH [46,74].

At Baggs farm, soil had higher EC during the early growing season (604 ± 71), which decreased to 418 ± 72 µS cm^{-1} in the midseason, and to 275 ± 31 µS cm^{-1} in the late growing season. Maximum soil EC was recorded at the upper slope (459 ± 63 µS cm^{-1}), followed by the toeslope (427 ± 65 µS cm^{-1}), and the middle slope (412 ± 47 µS cm^{-1}) (Figure 2e). At Research North, among the different slope positions, the middle slope had the maximum soil EC (320 ± 34 µS cm^{-1}), followed by the toeslope (297 ± 36 µS cm^{-1}), the upper (247 ± 34 µS cm^{-1}) and lower slope (237 ± 26 µS cm^{-1}). During the early growing season, soil EC was 444 ± 37 µS cm^{-1}, which decreased to 267 ± 44 µS cm^{-1} in the midseason and to 114 ± 16 µS cm^{-1} in the late growing season (Figure 3e). Mean EC values were higher at the Baggs farm at all slope positions as compared to Research North which could be attributed to soil texture variations between the farms. Research North had more sand content (sand:silt:clay = 76%:18%:6%) than Baggs farm (sand:silt:clay = 59%:32%:8%). Soil texture plays a significant role in EC variations and fields with higher sand content generally have lower EC [48,78]. In addition to soil texture, soil water content, nutrients

and salt accumulation and plant nutrient uptake also impact EC which causes intraseason variations in soil EC at different plant growth stages [79–82].

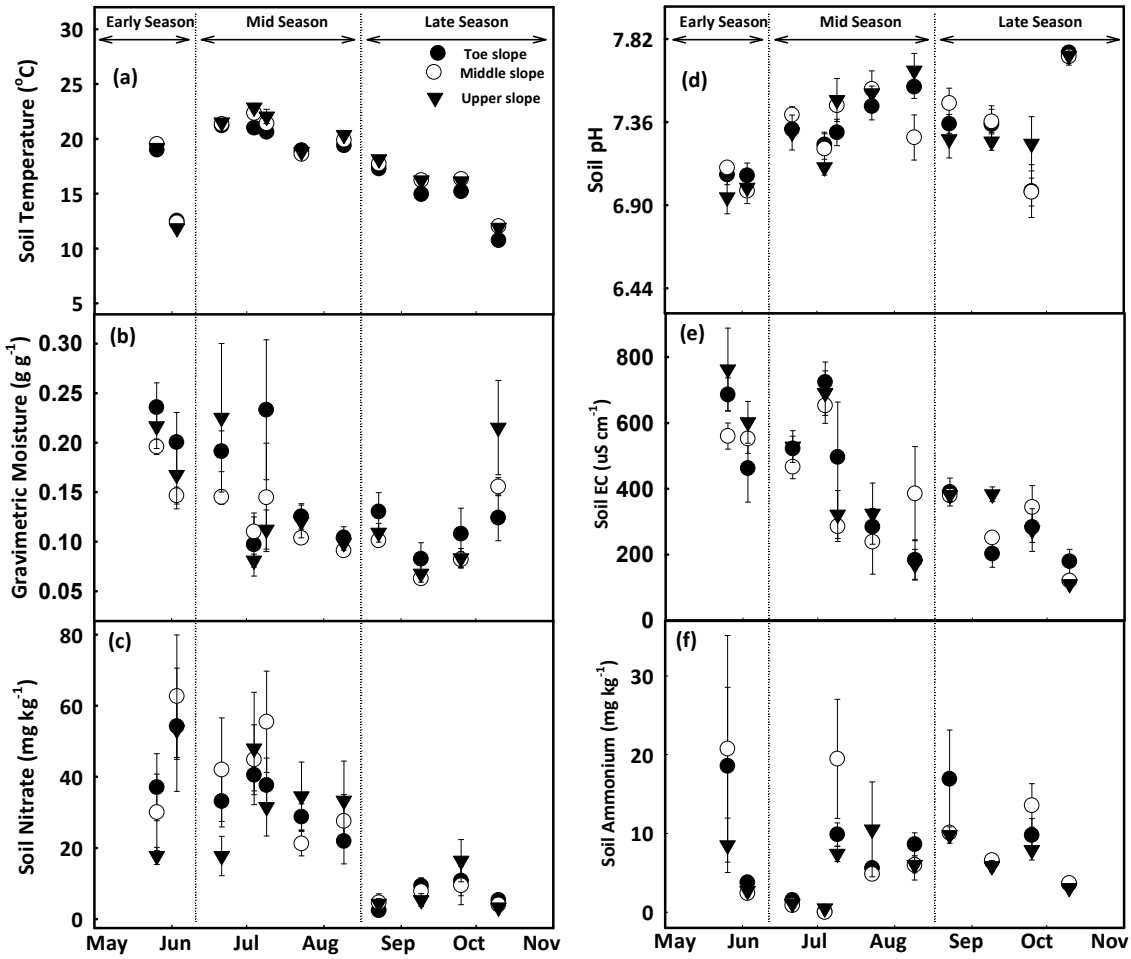

Figure 2. Temporal changes in soil temperature (**a**), gravimetric moisture content (**b**), nitrate (**c**), pH (**d**), electrical conductivity (**e**) and ammonium concentration (**f**) at Baggs farm. Scatter plots were prepared using mean values (Mean ± SEM) from four replications at each slope positions. Soil samples were collected during early season (26 May, 3 June), mid season (21 June, 4 July, 9 July, 23 July, 9 August) and late growing season (23 August, 9 September, 25 September, 10 October).

3.1.3. Nitrate and Ammonium Concentration

At Baggs farm, soil NO_3^- concentrations ranged from 2.4 ± 1 to 63 ± 17 mg kg^{-1} soil (Figure 2c) and maximum soil NO_3^- was recorded at the middle slope (30 ± 9 mg kg^{-1}), followed by the toeslope (28 ± 6 mg kg^{-1}), and upper slopes (25 ± 7 mg kg^{-1}) (Figure 2c). Soil had higher NO_3^- during the early growing season (42 ± 11 mg kg^{-1}), which decreased to 35 ± 9 mg kg^{-1} in the mid growing season, and further decreased to 7 ± 3 mg kg^{-1} in the late growing season (Figure 2c). At Research North, soil NO_3^- concentrations ranged from 0.06 ± 0.05 mg kg^{-1} soil to 34 ± 3 mg kg^{-1} (Figure 3c). On average, the maximum soil NO_3^- concentration was recorded at the middle slope (19 ± 5 mg kg^{-1}), followed by the upper (15 ± 4 mg kg^{-1}), toeslope (13 ± 4 mg kg^{-1}), and lower slope positions (10 ± 3 mg kg^{-1}) (Figure 3c). Soil had higher NO_3^- during the early growing season (19 ± 3 mg kg^{-1}), which decreased slightly to 17 ± 5 mg kg^{-1} in the mid growing season, and further decreased to 7 ± 3 mg kg^{-1} in the late growing season (Figure 3c). The upper slope position during the early (23 ± 3 mg kg^{-1}) and mid (18 ± 7 mg kg^{-1}) growing seasons while the middle slope position during the late growing season (15 ± 7 mg kg^{-1}) exhibited relatively higher NO_3^- concentrations than other slope positions (Figure 3c). At Baggs farm, the soil had higher NH_4^+ during the early growing season (9 ± 5 mg kg^{-1})

and that decreased to 5 ± 2 mg kg^{-1} in the mid growing season. In the late growing season, soil NH_4^+ increased to 8 ± 1 mg kg^{-1} (Figure 2f). On average, maximum soil NH_4^+ was observed at the middle slope (9 ± 3 mg kg^{-1}), followed by the toeslope (8 ± 3 mg kg^{-1}), and upper slope (6 ± 2 mg kg^{-1}) (Figure 2f). During the early and midseason, the middle slope had relatively higher NH_4^+ concentrations whereas this was true for the toeslope during the late growing season (Figure 2f). At Research North, higher soil NH_4^+ was recorded during the early season (26 ± 6 mg kg^{-1}), which decreased to 13 ± 6 mg kg^{-1} during the midseason and further decreased to 5 ± 0.5 mg kg^{-1} in the late growing season. Maximum soil NH_4^+ was observed at the upper slope (19 ± 6 mg kg^{-1}), followed by the middle (16 ± 5 mg kg^{-1}), toeslope (13 ± 3 mg kg^{-1}), and lower slope (10 ± 3 mg kg^{-1}) (Figure 3f).

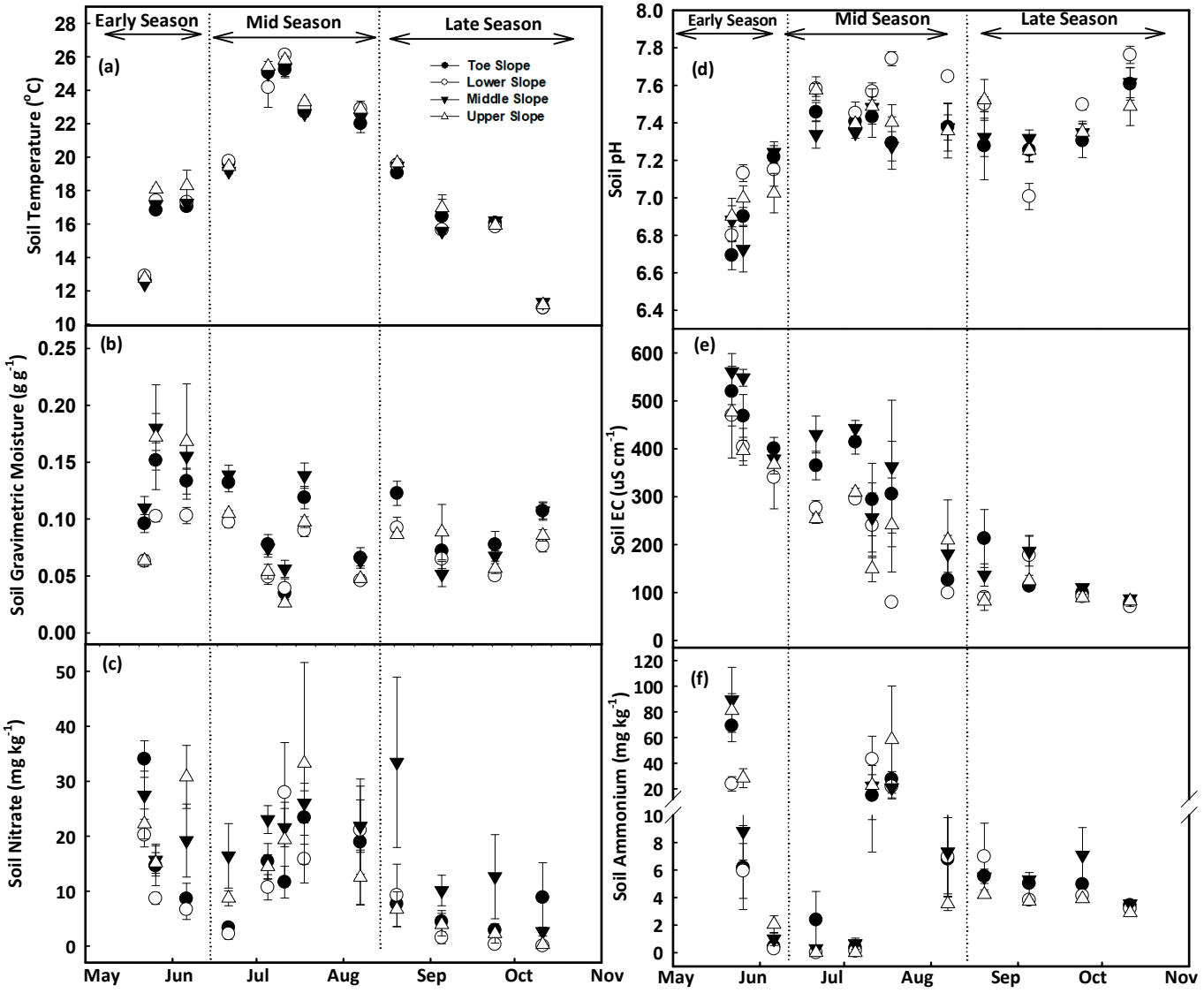

Figure 3. Temporal changes in soil temperature (**a**), gravimetric moisture content (**b**), nitrate (**c**), pH (**d**), electrical conductivity (**e**) and ammonium concentration (**f**) at Research North. Scatter plots were prepared using mean values (Mean ± SEM) from four replications at each slope positions. Soil samples were collected during early (22 May, 26 May, 6 June), mid (21 June, 5 July, 11 July, 18 July, 7 August), and the late growing season (20 August, 5 September, 24 September, 11 October).

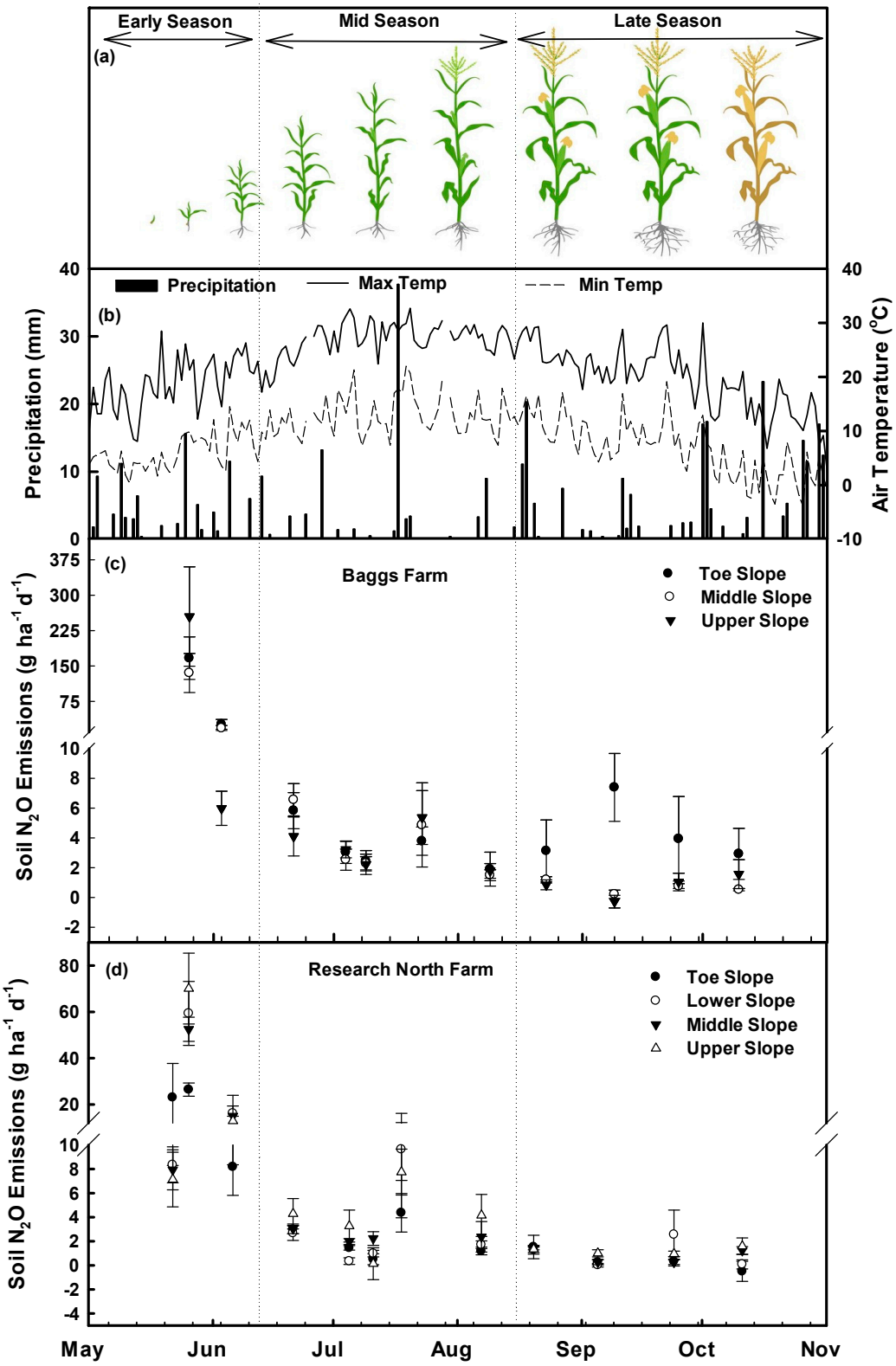

Figure 4. Corn growth seasons (**a**), weather conditions (**b**), and temporal patterns of Soil N_2O emissions at Baggs farm (**c**) and Research North (**d**). Scatter plots were prepared using mean N_2O emissions (Mean ± SEM) from four replications at each slope positions. Gas samples were collected from the Baggs farm during early season (26 May, 3 June), mid season (21 June, 4 July, 9 July, 23 July, 9 August) and late growing season (23 August, 9 September, 25 September, 10 October) and from Research North during early (22 May, 26 May, 6 June), mid (21 June, 5 July, 11 July, 18 July, 7 August), and the late growing season (20 August, 5 September, 24 September, 11 October). Image source [75].

Fertilizer application at planting increased soil NO_3^- and NH_4^+ concentration during the early growing season [83]. Over time, NO_3^- and NH_4^+ concentrations decreased due to plant uptake, nitrification, and/or losses in the form of leaching and NOx gasses [83,84]. Differential rates of mineralization and plant uptake due to moisture variations along landscape positions affected soil NO_3^- and NH_4^+ concentration within the field [30]. Rapid depletion of soil NH_4^+ and an increase of NO_3^- concentration during the early growing season at both farms could be due to higher nitrification rates [85]. Whereas a slower rate of soil NH_4^+ depletion was observed after the 2nd dose of N application as ATS is reported to decrease soil nitrification. This means NH_4^+ could stay in soil longer and remains available for plant uptake (Figure 2, Figure 3c,f) [86].

3.2. Nitrous Oxide Fluxes and Cumulative Emissions

Baggs farm: Different sampling dates during the early and mid growing seasons and slope positions during the late growing season had a significant impact ($p < 0.05$) on soil N_2O emissions (Table 1, Figure 4c). In the early growing season, N_2O emission peaks were observed immediately after corn planting, reaching up to 254 g N_2O ha^{-1} d^{-1} at the upper slope followed by 167 g N_2O ha^{-1} d^{-1} at the toeslope and 135 g N_2O ha^{-1} d^{-1} at the middle slope (Table 1). During the mid growing season, N_2O emissions decreased and the maximum N_2O emissions were recorded at 6.6 g N_2O ha^{-1} d^{-1} on 21 June at the middle slope. During the late growing season, the toeslope had higher N_2O emissions on all sampling dates, and the maximum emission (7.4 g N_2O ha^{-1} d^{-1}) was recorded on 9 September (Table 1). Over the entire growing season, toeslope, middle, and upper slope had higher N_2O emissions at 64%, 9%, and 27% of sampling dates, respectively (Table 1). High soil N_2O emissions were related to higher soil moisture (on 03 June, 09 July, 9 August, 23 August, 9 September), higher soil EC (on May 26, July 09, July 23, August 23, October 10), higher soil NO_3^- concentrations (on 21 June, 4 July, 23 July, 9 September, 10 October), and higher soil NH_4^+ concentrations (on 3 June, 4 July, 23 July, 9 August, 23 August) (Table 1, Figure 2). Maximum cumulative N_2O emissions were observed from the upper slope (1040 g N_2O ha^{-1}) during the early growing season, the middle slope (261 g N_2O ha^{-1}) during the mid growing season, and the toeslope (371 g N_2O ha^{-1}) during the late growing season (Table 2). Overall, 66% of the cumulative N_2O emissions occurred during the early growing season, 20% during the mid growing season and 14% during the late growing season which were in accordance with previous studies [87]. Among the slope positions, toeslope, middle, and upper slope positions emitted 37%, 26%, and 37% of the cumulative N_2O emissions over the whole growing season (Table 2).

Research North farm: At Research North, sampling dates had a significant impact on N_2O emissions ($p < 0.05$) during the early and mid growing season (Table 3). Maximum N_2O emissions were observed at the upper slope (70 $\pm$ 15 g N_2O ha^{-1} d^{-1}) on 26 May. Over the entire growing season, upper slope had higher N_2O emissions followed by toeslope, lower and middle slope at 50%, 17%, 17% and 16% of the sampling dates, respectively (Table 3). Higher soil N_2O emissions at individual dates were related to higher soil temperature (on 26 May, 6 June, 5 July, 7 August, 5 September, and 11 October), higher soil moisture (26 May, 11 July, 18 July, 20 August, 5 September and 11 October), lower soil pH (on 22 May, 18 July, 7 August, 20 August and 11 October), lower soil EC (on 26 May, 6 June, 21 June, 5 July, 5 September, 24 September and 11 October), lower soil NO_3^- (on 6 June, 7 August, 20 August, 5 September, 24 September, and 11 October), and low soil NH_4^+ concentration (on 6 June, 21 June, 5 July, 18 July, 7 August, 5 September, 24 September, and 11 October) (Table 3, Figure 3). Upper slope had maximum cumulative N_2O emissions to a value of 576 g N_2O ha^{-1}, 271 g N_2O ha^{-1} and 118 g N_2O ha^{-1} during the early, mid, and late growing season, respectively (Table 4). Overall, 58%, 28% and 13% of the total cumulative N_2O emissions were emitted during the early, mid, and late growing seasons, respectively. Among different slope positions, toeslope, lower, middle, and upper slope positions emitted 16%, 27%, 26%, and 31% of the total cumulative N_2O emissions (Table 4).

Overall, both farms emitted N_2O throughout the growing season and at all positions in the landscape except at the toeslope where on 11 October, the N_2O emission was -0.50 ± 0.83 g N_2O ha^{-1} at Research North and at the upper slope on 9 September when the N_2O emission was -0.27 ± 0.42 g N_2O ha^{-1} at the Baggs farm (Figure 4c,d). Fertilizer application increased soil NH_4^+ and NO_3^- concentrations (Figure 2 and Figure 3c,f) which increased nitrification and denitrification processes and N_2O emissions [87–94]. Higher overall N_2O emissions (Mean $\pm$ SE) were observed at the Baggs farm which could be attributed to variations in soil texture and greater variations in topography. Research North had more sand content (76%) than Baggs farm (59%) and sandy soils have been reported to emit less N_2O due to more soil aeration and less denitrification [95,96]. Similarly, the greater variations in topography at the Baggs farm could redistribute water quickly and could create variable hydrological conditions contributing to higher N_2O emissions. However, seasonal variations in soil drainage conditions might switch N_2O source depending on soil texture at various slope positions which caused temporal variations in N_2O emissions at different slope positions (Tables 1 and 3) [47,95].

Cumulative N_2O emissions over the growing season were moderate as compared to previous multi year trials [47,97–99], though, three times smaller than dairy manure based annual corn production [26,100]. Cumulative N_2O emissions during the early growing season were higher at both farms followed by the mid and late growing season. Urea application at planting increased soil inorganic N and N_2O emissions during the early growing season. Slope positions did not have a significant impact ($p > 0.05$) on cumulative N_2O emissions. However, higher cumulative N_2O emissions from the upper slope and lower emissions from the toeslope were recorded during the early, mid, and late growing season at Research North which could be attributed to higher soil NH_4^+ and soil temperatures than other positions (Figure 3). Higher temperatures at the upper slope could increase the expression of denitrification genes (nirS, cnorB) and increase N_2O emissions [101]. At the Baggs farm, upper slope during the early growing season, middle slope during the mid growing season and toeslope during the late growing season had higher cumulative N_2O emissions. Higher cumulative N_2O emissions from the upper slope during the early growing season might be due to relatively lower soil pH (6.97 ± 0.05) or higher soil EC (683 ± 94) (Figure 2). Soil pH has been reported as a master variable controlling denitrification rates and a high rate of N_2O emissions has been reported at near neutral pH [101–106]. During the mid growing season, middle slope had higher N_2O emissions which were not statistically different from other slope positions. These higher cumulative N_2O emissions may be triggered by higher soil NO_3^- and NH_4^+ concentrations at the middle slope (Figure 2). Soil NH_4^+ is converted to NO_3^- through nitrification, which is further converted to N_2O through the denitrification process [13,103]. During the late growing season, significantly higher cumulative N_2O emissions were reported from the toeslope which could result from higher soil volumetric content (data not presented), higher soil NH_4^+ and lower pH (Figure 2) [13,103].

Soil N_2O emissions have been reported to increase from the upper slope to the toeslope in various studies [53,54,107]. However, this pattern of N_2O emissions is not always the same under different field conditions [34]. For example, in this study, higher N_2O emissions were observed at the upper slope positions at Research North and different slope positions have varied responses over the early, mid, and late growing season at the Baggs farm (Tables 2 and 4). Different topographical positions influence soil hydrology and impact soil moisture, temperature, NO_3^-, NH_4^+, and organic C distribution in agricultural fields [34,108,109]. These variations could be attributed to local differences in the presence of previous crop residues at different slope positions and other topographical attributes, for example, contributing area, micro- depressions, water table depth, and curvature etc. [21,24,109,110] which require further investigation.

Topographical variations dictate spatial variations in soil properties and nutrient accumulation at different slope position during a crop growth period. These lead to varying spatial and temporal patterns of N_2O emissions over the crop growth period. Information

on the spatiotemporal variation of N_2O emission as controlled by topography over the crop growing season, thus must be considered in estimating agricultural contribution towards the annual emission, calculate emission factor and in developing agricultural management to mitigate climate change. For example, higher N_2O emissions were observed from the upper slope positions during the early growing season, and toeslope positions during the late growing season. Topography mediated nutrients and water redistribution from upper slope positions towards toeslope leads to spatial variations in soil IN and thus, N_2O emissions which could not be managed with traditional uniform fertilizer application methods. Precise application of N is required depending on crop demand and according to soil potential to hold IN depending on soil texture, moisture, pH, and CEC. Precision agricultural approaches combined with spatial variations in soil properties and N_2O emissions data from multiple studies could help to manage N_2O emissions at the landscape level.

4. Conclusions

Different crop growth periods (early, mid, and late growing season) had a significant impact on N_2O emissions. Various slope positions (toeslope, lower, middle, and upper) affected soil physico-chemical properties and large variations were observed within each slope position. Slope positions had a varied impact on temporal N_2O fluxes and cumulative N_2O emissions in different growing seasons. During the early growing season, crop management (fertilizer application and tillage) and environmental factors (soil moisture and temperature) affected soil biogeochemistry resulting in N_2O emission variations at different slope positions. Cumulative N_2O emissions during early growing season were as upper > middle > lower > toeslope. However, due to active vegetative growth during the mid growing season, topography does not seem to have an impact as the plants are continuously up taking water and available substrates for nitrification and denitrification. Nevertheless, during the late growing season, topography mediated hydrology and crop management does not really come into the picture as there is not enough water and nutrients in the soil. However, higher emissions were observed at the toeslope position and the cumulative emission pattern was toeslope > lower > upper > middle slope positions. However, due to large variations within different slope positions, further explorations into site-specific analysis of individual soil properties, including soil texture, SOM, Inorganic N dynamics, pH, EC, soil temperature, and moisture and their impact on N_2O emissions using multiyear data might help to understand the local hotspots for N_2O emissions. Nevertheless, the spatiotemporal variability in gas emissions as controlled by topography and crop growth stages can provide information to develop management strategies to mitigate agricultural impact on recent and future climate.

Author Contributions: A.B. and P.D. conceptualized the framework, funding acquisition and supervised the overall project; W.A. and H.B.V. collected sample and data, W.A. processed samples, analyzed data and wrote the manuscript; A.B. and P.D. edited the manuscript; P.D. and U.G. reviewed the final manuscript. All authors have read and agreed to the published version of the manuscript.

Funding: This work support by research grant from Natural Sciences and Engineering Research Council of Canada (NSERC) (RGPIN-2014-4100) and the Ontario Ministry of Agriculture Food and Rural Affairs (OMAFRA) University of Guelph project UofG 22017-2889.

Institutional Review Board Statement: This study did not involve humand or animals.

Conflicts of Interest: The authors declare no conflict of interest.

References

1. IPCC. *Climate Change 2007: The Physical Science Basis: Contribution of Working Group I to the Fourth Assessment Report of the Intergovernmental Panel on Climate Change*; Cambridge University Press: Cambridge, UK, 2007.
2. UNFCCC. Kyoto Protocol Reference Manual on Accounting of Emissions and Assigned Amount. Available online: https://unfccc.int/resource/docs/publications/08_unfccc_kp_ref_manual.pdf (accessed on 20 September 2020).

3. UNFCCC. Kyoto Protocol to the United Nations Framework Convention on Climate Change. Available online: https://unfccc.int/resource/docs/convkp/kpeng.pdf (accessed on 20 September 2020).
4. UNFCCC. Paris Agreement. Available online: https://unfccc.int/process-and-meetings/the-paris-agreement/the-paris-agreement (accessed on 20 September 2020).
5. IPCC. Climate Change and Land: An IPCC Special Report on Climate Change, Desertification, Land Degradation, Sustainable Land Management, Food Security, and Greenhouse Gas Fluxes in Terrestrial Ecosystems: Summary for Policymakers. Available online: https://www.ipcc.ch/site/assets/uploads/2019/11/SRCCL-Full-Report-Compiled-191128.pdf (accessed on 20 September 2020).
6. FAO. Agriculture, Forestry and Other Land Use Emissions by Sources and Removals by Sinks; Tubiello, F.N., Salvatore, M., Cóndor Golec, R.D., Ferrara, A., Rossi, S., Biancalani, R., Federici, S., Jacobs, H., Flammini, A., Eds. Available online: http://www.fao.org/docrep/019/i3671e/i3671e.pdf (accessed on 20 September 2020).
7. Environment and Climate Change Canada. National Inventory Report 1996–2016: Greenhouse Gas Sources and Sinks in Canada. Available online: http://publications.gc.ca/collections/collection_2018/eccc/En81-4-2016-3-eng.pdf (accessed on 20 September 2020).
8. Abdalla, M.; Osborne, B.; Lanigan, G.; Forristal, D.; Williams, M.; Smith, P.; Jones, M.B. Conservation tillage systems: A review of its consequences for greenhouse gas emissions. *Soil. Use Manag.* **2013**, *29*, 199–209. [CrossRef]
9. Congreves, K.A.; Wagner-Riddle, C.; Si, B.C.; Clough, T.J. Nitrous oxide emissions and biogeochemical responses to soil freezing-thawing and drying-wetting. *Soil Biol. Biochem.* **2018**, *117*, 5–15. [CrossRef]
10. Decock, C. Mitigating nitrous oxide emissions from corn cropping systems in the midwestern U.S.: Potential and data gaps. *Environ. Sci. Technol.* **2014**, *48*, 4247–4256. [CrossRef]
11. FAO. Greenhouse Gas Emissions from Agriculture, Forestory and Other Land Use. Available online: http://www.fao.org/resources/infographics/infographics-details/en/c/218650/ (accessed on 20 September 2020).
12. Wrage-Mönnig, N.; Horn, M.A.; Well, R.; Müller, C.; Velthof, G.; Oenema, O. The role of nitrifier denitrification in the production of nitrous oxide revisited. *Soil Biol. Biochem.* **2018**, *123*, A3–A16. [CrossRef]
13. Moreira, F.M.S.; Siqueira, J.O. *Microbiology and Soil Biochemistry*; Federal University of Lavras: Lavras, Brazil, 2006; Volume 2.
14. Signor, D.; Cerri, C.E.P. Nitrous oxide emissions in agricultural soils: A review. *Pesqui. Agropecu. Trop. Goia.* **2013**, *43*, 322–338. [CrossRef]
15. Oertel, C.; Matschullat, J.; Zurba, K.; Zimmermann, F.; Erasmi, S. Greenhouse gas emissions from soils—A review. *Chem. Erde* **2016**, *76*, 327–352. [CrossRef]
16. Butterbach-Bahl, K.; Baggs, E.M.; Dannenmann, M.; Kiese, R.; Zechmeister-Boltenstern, S. Nitrous oxide emissions from soils: How well do we understand the processes and their controls? *Philos. Trans. R. Soc. B Biol. Sci.* **2013**, *368*, 20130122. [CrossRef] [PubMed]
17. Pimentel, L.G.; Weiler, D.A.; Pedroso, G.M.; Bayer, C. Soil N_2O emissions following cover-crop residues application under two soil moisture conditions. *J. Plant Nutr. Soil Sci.* **2015**, *178*, 631–640. [CrossRef]
18. Rücknagel, J.; Rademacher, A.; Götze, P.; Hofmann, B.; Christen, O. Uniaxial compression behaviour and soil physical quality of topsoils under conventional and conservation tillage. *Geoderma* **2017**, *286*, 1–7. [CrossRef]
19. Stewart, K.J.; Grogan, P.; Coxson, D.S.; Siciliano, S.D. Topography as a key factor driving atmospheric nitrogen exchanges in arctic terrestrial ecosystems. *Soil Biol. Biochem.* **2014**, *70*, 96–112. [CrossRef]
20. Corre, M.D.; van Kessel, C.; Pennock, D.J. Landscape and Seasonal Patterns of Nitrous Oxide Emissions in a Semiarid Region. *Soil Sci. Soc. Am. J.* **1996**, *60*, 1806–1815. [CrossRef]
21. Gu, J.; Nicoullaud, B.; Rochette, P.; Pennock, D.J.; Hénault, C.; Cellier, P.; Richard, G. Effect of topography on nitrous oxide emissions from winter wheat fields in Central France. *Environ. Pollut.* **2011**, *159*, 3149–3155. [CrossRef]
22. Vilain, G.; Garnier, J.; Tallec, G.; Cellier, P. Effect of slope position and land use on nitrous oxide (N2O) emissions (Seine Basin, France). *Agric. For. Meteorol.* **2010**, *150*, 1192–1202. [CrossRef]
23. Vilain, G.; Garnier, J.; Passy, P.; Silvestre, M.; Billen, G. Budget of N_2O emissions at the watershed scale: Role of land cover and topography (the Orgeval basin, France). *Biogeosciences* **2012**, *9*, 1085–1097. [CrossRef]
24. Izaurralde, R.C.; Lemke, R.L.; Goddard, T.W.; McConkey, B.; Zhang, Z. Nitrous oxide emissions from agricultural toposequences in Alberta and Saskatchewan. *Soil Sci. Soc. Am. J.* **2004**, *68*, 1285. [CrossRef]
25. Saggar, S.; Giltrap, D.L.; Davison, R.; Gibson, R.; de Klein, C.A.M.; Rollo, M.; Ettema, P.; Rys, G. Estimating direct N_2O emissions from sheep, beef, and deer grazed pastures in New Zealand hill country: Accounting for the effect of land slope on the N_2O emission factors from urine and dung. *Agric. Ecosyst. Environ.* **2015**, *205*, 70–78. [CrossRef]
26. Ashiq, W.; Nadeem, M.; Ali, W.; Zaeem, M.; Wu, J.; Galagedara, L.; Thomas, R.; Kavanagh, V.; Cheema, M. Biochar amendment mitigates greenhouse gases emission and global warming potential in dairy manure based silage corn in boreal climate. *Environ. Pollut.* **2020**, *265*, 114869. [CrossRef] [PubMed]
27. Parkin, T.B.; Kaspar, T.C. Nitrous Oxide Emissions from Corn–Soybean Systems in the Midwest. *J. Environ. Qual.* **2006**, *35*, 1496. [CrossRef]
28. Liu, X.J.; Mosier, A.R.; Halvorson, A.D.; Zhang, F.S. The impact of nitrogen placement and tillage on NO, N2O, CH4 and CO2 fluxes from a clay loam soil. *Plant Soil* **2006**, *280*, 177–188. [CrossRef]
29. Wang, Z.M.; Zhang, B.; Song, K.S.; Liu, D.W.; Li, F.; Guo, Z.X.; Zhang, S.M. Soil organic carbon under different landscape attributes in croplands of Northeast China. *Plant, Soil Environ.* **2008**, *54*, 420–427. [CrossRef]

30. Noorbakhsh, S.; Schoenau, J.; Si, B.; Zeleke, T.; Qian, P. Soil properties, yield, and landscape relationships in south-central Saskatchewan Canada. *J. Plant Nutr.* **2008**, *31*, 539–556. [CrossRef]
31. Moges, A.; Holden, N.M. Soil fertility in relation to slope position and agricultural land use: A case study of umbulo catchment in Southern Ethiopia. *Environ. Manag.* **2008**, *42*, 753–763. [CrossRef] [PubMed]
32. Ladoni, M.; Kravchenko, A.N.; Phillip Robertson, G. Topography mediates the influence of cover crops on soil nitrate levels in row crop agricultural systems. *PLoS ONE* **2015**, *10*, e0143358. [CrossRef] [PubMed]
33. Gaultier, J.; Farenhorst, A.; Crow, G. Spatial variability of soil properties and 2,4-D sorption in a hummocky field as affected by landscape position and soil depth. *Can. J. Soil Sci.* **2006**, *86*, 89–95. [CrossRef]
34. Arias-Navarro, C.; Díaz-Pinés, E.; Klatt, S.; Brandt, P.; Rufino, M.C.; Butterbach-Bahl, K.; Verchot, L.V. Spatial variability of soil N2O and CO2 fluxes in different topographic positions in a tropical montane forest in Kenya. *J. Geophys. Res. Biogeosci.* **2017**, *122*, 514–527. [CrossRef]
35. Norton, J.B.; Sandor, J.A.; White, C.S. Hillslope Soils and Organic Matter Dynamics within a Native American Agroecosystem on the Colorado Plateau. *Soil Sci. Soc. Am. J.* **2003**, *67*, 225–234. [CrossRef]
36. Wang, J.; Fu, B.; Qiu, Y.; Chen, L. Soil nutrients in relation to land use and landscape position in the semi-arid small catchment on the loess plateau in China. *J. Arid Environ.* **2001**, *48*, 537–550. [CrossRef]
37. Jowkin, V.; Schoenau, J.J. Impact of tillage and landscape position on nitrogen availability and yield of spring wheat in the Brown soil zone in southwestern Saskatchewan. *Can. J. Soil Sci.* **1998**, *78*, 563–572. [CrossRef]
38. Burke, I.C.; Elliott, E.T.; Cole, C.V. Influence of Macroclimate, Landscape Position, and Management on Soil Organic Matter in Agroecosystems. *Ecol. Appl.* **1995**, *5*, 124–131. [CrossRef]
39. Mulla, F.B.; Pierson, D.J. Aggregate Stability in the Palouse Region of Washington: Effect of Landscape Position. *Soil Sci. Soc. Am. J.* **1990**, *54*, 1407–1412.
40. Hook, P.B.; Bruke, I.C. Biogeochemistry in a shortgrass landscape: Control by topography, soil texture, and microclimate. *Ecology* **2000**, *81*, 2686–2703. [CrossRef]
41. IPCC. IPCC Expert Meeting for Technical Assessment of IPCC Inventory Guidelines (AFOLU Sector). Available online: https://www.ipcc.ch/site/assets/uploads/2018/05/1604_Summary_TA-followup-2015issues.pdf (accessed on 20 September 2020).
42. IPCC. N2O Emissions from Managed Soils, and CO2 Emissions from Lime and Urea Application. Available online: https://www.ipccnggip.iges.or.jp/public/2006gl/pdf/4_Volume4/V4_11_Ch11_N2O&CO2.pdf (accessed on 20 September 2020).
43. Biswas, A.; Chau, H.W.; Bedard-Haughn, A.K.; Si, B.C. Factors controlling soil water storage in the hummocky landscape of the Prairie Pothole Region of North America. *Can. J. Soil Sci.* **2012**, *92*, 649–663. [CrossRef]
44. Li, X.; Mccarty, G.W.; Lang, M.; Ducey, T.; Hunt, P.; Miller, J. Topographic and physicochemical controls on soil denitrification in prior converted croplands located on the Delmarva Peninsula, USA. *Geoderma* **2018**, *309*, 41–49. [CrossRef]
45. Franzen, D.W.; Nanna, T.; Norvell, W.A. A survey of soil attributes in North Dakota by landscape position. *Agron. J.* **2006**, *98*, 1015–1022. [CrossRef]
46. Yimer, F.; Ledin, S.; Abdelkadir, A. Soil property variations in relation to topographic aspect and vegetation community in the south-eastern highlands of Ethiopia. *For. Ecol. Manag.* **2006**, *232*, 90–99. [CrossRef]
47. Gregorich, E.G.; Rochette, P.; St-Georges, P.; McKim, U.F.; Chan, C. Tillage effects on N2O emission from soils under corn and soybeans in Eastern Canada. *Can. J. Soil Sci.* **2008**, *88*, 153–161. [CrossRef]
48. Stadler, A.; Rudolph, S.; Kupisch, M.; Langensiepen, M.; van der Kruk, J.; Ewert, F. Quantifying the effects of soil variability on crop growth using apparent soil electrical conductivity measurements. *Eur. J. Agron.* **2015**, *64*, 8–20. [CrossRef]
49. Jenny, H. *Factors of Soil Formation: A System of Quantitative Pedology*; Courier Corporation: North Chelmsford, MA, USA, 1994.
50. Biswas, A.; Si, B.C. Scales and locations of time stability of soil water storage in a hummocky landscape. *J. Hydrol.* **2011**, *408*, 100–112. [CrossRef]
51. Pennock, D.J. Terrain attributes, landform segmentation, and soil redistribution. *Soil Tillage Res.* **2003**, *69*, 15–26. [CrossRef]
52. Pennock, D.J.; Anderson, D.W.; de Jong, E. Landscape-scale changes in indicators of soil quality due to cultivation in Saskatchewan, Canada. *Geoderma* **1994**, *64*, 1–19. [CrossRef]
53. Fang, Y.; Gundersen, P.; Zhang, W.; Zhou, G.; Christiansen, J.R.; Mo, J.; Dong, S.; Zhang, T. Soil-atmosphere exchange of N2O, CO2 and CH4 along a slope of an evergreen broad-leaved forest in southern China. *Plant Soil* **2009**, *319*, 37–48. [CrossRef]
54. Dunmola, A.S.; Tenuta, M.; Moulin, A.P.; Yapa, P.; Lobb, D.A. Pattern of greenhouse gas emission from a Prairie Pothole agricultural landscape in Manitoba, Canada. *Can. J. Soil Sci.* **2010**, *90*, 243–256. [CrossRef]
55. Li, J.; Anderson, T.; Walter, M.T. Landscape scale variation in nitrous oxide flux along a typical northeastern US topographic gradient in the early summer. *Water. Air. Soil Pollut.* **2012**, *223*, 1571–1580. [CrossRef]
56. Yates, T.T.; Si, B.C.; Farrell, R.E.; Pennock, D.J. Time, location, and scale dependence of soil nitrous oxide emissions, soil water, and temperature using wavelets, cross-wavelets, and wavelet coherency analysis. *J. Geophys. Res. Atmos.* **2007**, *112*, D9. [CrossRef]
57. Luo, J.; Hoogendoorn, C.; van der Weerden, T.; Saggar, S.; de Klein, C.; Giltrap, D.; Rollo, M.; Rys, G. Nitrous oxide emissions from grazed hill land in New Zealand. *Agric. Ecosyst. Environ.* **2013**, *181*, 58–68. [CrossRef]
58. Pennock, D.J.; Zebarth, B.J.; De Jong, E. Landform classification and soil distribution in hummocky terrain, Saskatchewan, Canada. *Geoderma* **1987**, *40*, 297–315. [CrossRef]
59. Pringle, G. Maize production: Managing critical plant growth stages Available online:. Available online: https://www.farmersweekly.co.za/crops/field-crops/maize-production-managing-critical-plant-growth-stages/ (accessed on 20 September 2020).

60. Cambareri, G.; Wagner-Riddle, C.; Drury, C.; Lauzon, J.; Salas, W. Anaerobically digested dairy manure as an alternative nitrogen source to mitigate nitrous oxide emissions in fall-fertilized corn. *Can. J. Soil Sci.* **2016**, *97*, 439–451. [CrossRef]
61. Collier, S.M.; Ruark, M.D.; Oates, L.G.; Jokela, W.E.; Dell, C.J. Measurement of greenhouse gas flux from agricultural soils using static chambers. *J. Vis. Exp.* **2014**, e52110. [CrossRef]
62. Ferrari Machado, P.V.; Wagner-Riddle, C.; MacTavish, R.; Voroney, P.R.; Bruulsema, T.W. Diurnal Variation and Sampling Frequency Effects on Nitrous Oxide Emissions Following Nitrogen Fertilization and Spring-Thaw Events. *Soil Sci. Soc. Am. J.* **2019**, *83*, 743. [CrossRef]
63. Cambareri, G.; Drury, C.; Lauzon, J.; Salas, W.; Wagner-Riddle, C. Year-round nitrous oxide emissions as affected by timing and method of dairy manure application to corn. *Soil Sci. Soc. Am. J.* **2017**, *81*, 166–178. [CrossRef]
64. Fassbinder, J.J.; Schultz, N.M.; Baker, J.M.; Griffis, T.J. Automated, low-power chamber system for measuring nitrous oxide emissions. *J. Environ. Qual.* **2013**, *42*, 606–614. [CrossRef] [PubMed]
65. Carter, M.R.; Gregorich, E.G. *Soil Sampling and Methods of Analysis*, 2nd ed.; Gregorich, M.R.C.E.G., Ed.; Taylor & Francis: Roca Raton, FL, USA, 2008.
66. Yang, X.; Lan, Y.; Meng, J.; Chen, W.; Huang, Y.; Cheng, X.; He, T.; Cao, T.; Liu, Z.; Jiang, L.; et al. Effects of maize stover and its derived biochar on greenhouse gases emissions and C-budget of brown earth in Northeast China. *Environ. Sci. Pollut. Res.* **2017**, *24*, 8200–8209. [CrossRef] [PubMed]
67. Menéndez, S.; Merino, P.; Pinto, M.; González-Murua, C.; Estavillo, J.M. 3,4-Dimethylpyrazol phosphate effect on nitrous oxide, nitric oxide, ammonia, and carbon dioxide emissions from grasslands. *J. Environ. Qual.* **2006**, *35*, 973–981. [CrossRef] [PubMed]
68. Cai, Y.; Ding, W.; Luo, J. Nitrous oxide emissions from Chinese maize-wheat rotation systems: A 3-year field measurement. *Atmos. Environ.* **2013**, *65*, 112–122. [CrossRef]
69. Agbenin, J.O.; Tiessen, H. Soil properties and their variations on two contiguous hillslopes in Northeast Brazil. *Catena* **1995**, *24*, 147–161. [CrossRef]
70. Luo, G.J.; Kiese, R.; Wolf, B.; Butterbach-Bahl, K. Effects of soil temperature and moisture on methane uptake and nitrous oxide emissions across three different ecosystem types. *Biogeosciences* **2013**, *10*, 3205–3219. [CrossRef]
71. Sanchez, P.A. *Properties and management of soils in the tropics*; Cambridge University Press: Cambridge, uk, 2019.
72. Whitson, I.R. Hydropedology of depression-toe slope interaction across a soil unit boundary at the Boreal-Prairie interface. *Catena* **2020**, *187*, 104349. [CrossRef]
73. VandenBygaart, A.J. Erosion and deposition history derived by depth-stratigraphy of 137Cs and soil organic carbon. *Soil Tillage Res.* **2001**, *61*, 187–192. [CrossRef]
74. Papiernik, S.K.; Schumacher, T.E.; Lobb, D.A.; Lindstrom, M.J.; Lieser, M.L.; Eynard, A.; Schumacher, J.A. Soil properties and productivity as affected by topsoil movement within an eroded landform. *Soil Tillage Res.* **2009**, *102*, 67–77. [CrossRef]
75. VectorStock Media Growth Stages of Maize Plant Corn Phases. Available online: https://www.vectorstock.com/royalty-free-vector/growth-stages-of-maize-plant-corn-phases-vector-24284737 (accessed on 8 September 2020).
76. Rochette, P.; Angers, D.A.; Chantigny, M.H.; Gasser, M.O.; MacDonald, J.D.; Pelster, D.E.; Bertrand, N. NH3 volatilization, soil NH4+concentration and soil pH following subsurface banding of urea at increasing rates. *Can. J. Soil Sci.* **2013**, *93*, 261–268. [CrossRef]
77. Sommer, S.G.; Schjoerring, J.K.; Denmead, O.T. Ammonia emission from mineral fertilizers and fertilized crops. *Adv. Agron.* **2004**, *82*, 557–622.
78. Guo, W.; Maas, S.J.; Bronson, K.F. Relationship between cotton yield and soil electrical conductivity, topography, and Landsat imagery. *Precis. Agric.* **2012**, *13*, 678–692. [CrossRef]
79. Ejaz, S.; Jezik, K.M.; Stumpf, W.; Gosch, C.; Halbwirth, H.; Stich, K. Amelioration of an open soilless cultivation system for microgardening spinach (*Spinacia oleracea* L.). *Zemdirbyste-Agriculture* **2015**, *102*, 201–208. [CrossRef]
80. Brevik, E.C.; Fenton, T.E.; Lazari, A. Soil electrical conductivity as a function of soil water content and implications for soil mapping. *Precis. Agric.* **2006**, *7*, 393–404. [CrossRef]
81. Ding, Y.; Liu, Y.X.; Wu, W.X.; Shi, D.Z.; Yang, M.; Zhong, Z.K. Evaluation of biochar effects on nitrogen retention and leaching in multi-layered soil columns. *Water. Air. Soil Pollut.* **2010**, *213*, 47–55. [CrossRef]
82. de Andrade Neto, T.M.; Coelho, E.F.; Silva, A.C.P. Calcium nitrate concentrations in fertigation for "terra" banana production. *J. Brazilian Assoc. Agric. Eng.* **2017**, *37*, 385–393. [CrossRef]
83. Kabala, C.; Karczewska, A.; Gałka, B.; Cuske, M.; Sowiński, J. Seasonal dynamics of nitrate and ammonium ion concentrations in soil solutions collected using MacroRhizon suction cups. *Environ. Monit. Assess.* **2017**, *189*. [CrossRef]
84. Jones, R.W.; Hedlin, R.A. Ammonium, nitrite and nitrate accumulation in three Manitoba soils as influenced by added ammonium sulfate and urea. *Can. J. Soil Sci.* **1970**, *50*, 331–338. [CrossRef]
85. Qian, C.; Cai, Z. Leaching of nitrogen from subtropical soils as affected by nitrification potential and base cations. *Plant Soil* **2007**, *300*, 197–205. [CrossRef]
86. Kugler Company. Ammonium Thiosulfate as a Nitrogen Source and Nitrogen Inhibitor. Available online: http://www.kuglercompany.com/products/ats-ammonium-thiosulfate (accessed on 20 September 2020).
87. Rochette, P.; Angers, D.A.; Chantigny, M.H.; Gagnon, B.; Bertrand, N. N2O fluxes in soils of contrasting textures fertilized with liquid and solid dairy cattle manures. *Can. J. Soil Sci.* **2008**, *88*, 175–187. [CrossRef]

88. Zhai, L. mei; Liu, H. bin; Zhang, J. zong; Huang, J.; Wang, B. ren Long-term application of organic manure and mineral fertilizer on N2O and CO2 emissions in a red soil from cultivated maize-wheat rotation in China. *Agric. Sci. China* **2011**, *10*, 1748–1757. [CrossRef]
89. Ruser, R.; Flessa, H.; Russow, R.; Schmidt, G.; Buegger, F.; Munch, J.C. Emission of N2O, N2 and CO2 from soil fertilized with nitrate: Effect of compaction, soil moisture and rewetting. *Soil Biol. Biochem.* **2006**, *38*, 263–274. [CrossRef]
90. Sun, Z.; Sänger, A.; Rebensburg, P.; Lentzsch, P.; Wirth, S.; Kaupenjohann, M.; Meyer-Aurich, A. Contrasting effects of biochar on N2O emission and N uptake at different N fertilizer levels on a temperate sandy loam. *Sci. Total Environ.* **2017**, *578*, 557–565. [CrossRef] [PubMed]
91. Lutes, K.; Oelbermann, M.; Thevathasan, N.V.; Gordon, A.M. Effect of nitrogen fertilizer on greenhouse gas emissions in two willow clones (Salix miyabeana and S. dasyclados) in southern Ontario, Canada. *Agrofor. Syst.* **2016**, *90*, 785–796. [CrossRef]
92. Lan, T.; Li, M.; Han, Y.; Deng, O.; Tang, X.; Luo, L.; Zeng, J.; Chen, G.; Yuan, S.; Wang, C.; et al. How are annual CH4, N2O, and NO emissions from rice–wheat system affected by nitrogen fertilizer rate and type? *Appl. Soil Ecol.* **2020**, *150*, 103469. [CrossRef]
93. Inselsbacher, E.; Wanek, W.; Ripka, K.; Hackl, E.; Sessitsch, A.; Strauss, J.; Zechmeister-Boltenstern, S. Greenhouse gas fluxes respond to different N fertilizer types due to altered plant-soil-microbe interactions. *Plant Soil* **2011**, *343*, 17–35. [CrossRef]
94. Kostyanovsky, K.I.; Huggins, D.R.; Stockle, C.O.; Morrow, J.G.; Madsen, I.J. Emissions of N2O and CO2 following short-term water and N fertilization events in wheat-based cropping systems. *Front. Ecol. Evol.* **2019**, *7*, 77241. [CrossRef]
95. Skiba, U.; Ball, B. The effect of soil texture and soil drainage on emissions of nitric oxide and nitrous oxide. *Soil Use Manag.* **2002**, *18*, 56–60. [CrossRef]
96. Syväsalo, E.; Regina, K.; Pihlatie, M.; Esala, M. Emissions of nitrous oxide from boreal agricultural clay and loamy sand soils. *Nutr. Cycl. Agroecosystems* **2004**, *69*, 155–165. [CrossRef]
97. Roy, A.K.; Wagner-Riddle, C.; Deen, B.; Lauzon, J.; Bruulsema, T. Nitrogen application rate, timing and history effects on nitrous oxide emissions from corn (*Zea mays* L.). *Can. J. Soil Sci.* **2014**, *94*, 563–573. [CrossRef]
98. Wagner-riddle, C.; Furon, A.; Mclaughlin, N.L.; Lee, I.; Barbeau, J.; Jayasundara, S.; Parkin, G.; von Bertoldi, P.; Warland, J. Intensive measurement of nitrous oxide emissions from a corn-soybean-wheat rotation under two contrasting management systems over 5 years. *Glob. Chang. Biol.* **2007**, *13*, 1722–1736. [CrossRef]
99. Hyatt, C.R.; Venterea, R.T.; Rosen, C.J.; McNearney, M.; Wilson, M.L.; Dolan, M.S. Polymer-Coated Urea Maintains Potato Yields and Reduces Nitrous Oxide Emissions in a Minnesota Loamy Sand. *Soil Sci. Soc. Am. J.* **2010**, *74*, 419–428. [CrossRef]
100. Abalos, D.; Brown, S.E.; Vanderzaag, A.C.; Gordon, R.J.; Dunfield, K.E.; Wagner-Riddle, C. Micrometeorological measurements over 3 years reveal differences in N2O emissions between annual and perennial crops. *Glob. Chang. Biol.* **2016**, *22*, 1244–1255. [CrossRef] [PubMed]
101. Saleh-Lakha, S.; Shannon, K.E.; Henderson, S.L.; Goyer, C.; Trevors, J.T.; Zebarth, B.J.; Burton, D.L. Effect of pH and temperature on denitrification gene expression and activity in Pseudomonas mandelii. *Appl. Environ. Microbiol.* **2009**, *75*, 3903–3911. [CrossRef] [PubMed]
102. Simek, M.; Cooper, J.E. The influence of soil pH on denitrification: Progress towards the understanding of this interaction over the last 50 years. *Eur. J. Soil Sci.* **2002**, *53*, 345–354. [CrossRef]
103. Thomas, K.L.; Lloyd, D.; Boddy, L. Effects of oxygen, pH and nitrate concentration on denitrification by Pseudomonas species. *FEMS Microbiol. Lett.* **1994**, *118*, 181–186. [CrossRef] [PubMed]
104. Thomsen, J.K.; Geest, T.; Cox, R.P. Mass spectrometric studies of the effect of pH on the accumulation of intermediates in denitrification by Paracoccus denitrificans. *Appl. Environ. Microbiol.* **1994**, *60*, 536–541. [CrossRef]
105. Valera, C.L.; Alexander, M. Nutrition and physiology of denitrifying bacteria. *Plant Soil* **1961**, *15*, 268–280. [CrossRef]
106. Van Den Heuvel, R.N.; Bakker, S.E.; Jetten, M.S.M.; Hefting, M.M. Decreased N2O reduction by low soil pH causes high N2O emissions in a riparian ecosystem. *Geobiology* **2011**, *9*, 294–300. [CrossRef]
107. Saha, D.; Rau, B.M.; Kaye, J.P.; Montes, F. Landscape control of nitrous oxide emissions during the transition from conservation reserve program to perennial grasses for bioenergy. *GCB Bioenergy* **2017**, *9*, 783–795. [CrossRef]
108. Pennock, D.; Yates, T.; Bedard-haughn, A.; Phipps, K.; Farrell, R.; Mcdougal, R. Landscape controls on N 2 O and CH 4 emissions from freshwater mineral soil wetlands of the Canadian Prairie Pothole region. *Geoderma* **2010**, *155*, 308–319. [CrossRef]
109. Han, Z.; Walter, M.T.; Drinkwater, L.E. Impact of cover cropping and landscape positions on nitrous oxide emissions in northeastern US agroecosystems. *Agric. Ecosyst. Environ.* **2017**, *245*, 124–134. [CrossRef]
110. Pennock, D.; Farrell, R.; Desjardins, R.; Pattey, E.; MacPherson, J.I.I. Upscaling chamber-based measurements of N2O emissions at snowmelt. *Can. J. Soil Sci.* **2005**, *85*, 113–125. [CrossRef]